REVIEW

Mesoporous materials in sensing: morphology and functionality at the meso-interface

Brian J. Melde · Brandy J. Johnson

Abstract Mesoporous materials are finding increasing utility in sensing applications. These applications can benefit from a surface area that may exceed 1,000 m^2 g^{-1} and fast diffusion of analytes through a porous structure. This article reviews recent developments in mesoporous materials-based sensing and provides examples of the impact of different surface functionality, pore structure, and macro-morphology in an attempt to illustrate the contribution of these factors to the selectivity and sensitivity of a sensor response. The materials discussed include ordered mesoporous silicates synthesized with surfactants, hard templated ordered mesoporous carbons, and metal oxides with porous textures which have been applied to advantage in various detection schemes. Chemical functionalization of mesoporous materials through silane grafting, co-condensation, and adsorption are also addressed.

Keywords Mesopore · Micropore · Morphology · Surfactant-template · Imprint · Metal oxide

Introduction

The basic components necessary to any sensing system are the recognition element, the transducer, and the detector. The recognition element is the component of the sensor that interacts with the target. The transducer converts interaction with the target into a signal that is measured by the detector. Depending on the sensor system, the recognition element may also act as the transducer. Detection is accomplished by one of a few established methods, for example electrochemical, optical, or acoustic. A large component of ongoing work in the development of sensors is related to recognition and transduction elements. Effort is focused on the development of elements with higher sensitivity or selectivity, more rapid response characteristics, broader working ranges, and improved reusability. In applications employing mesoporous materials, many of these desirable traits are related to the interface between the material and target. The characteristics of this interface can be affected by a number of factors. Application of mesoporous materials can involve their use as scaffolds for immobilization of receptors, for which morphology is a primary concern, or synthesis of surfaces which have desirable binding characteristics, shifting the focus to functional group distribution. This review focuses on recent reports of selective sensing applications utilizing mesoporous surfaces. The emphasis is on examples in which interactions at the surface and/or pore geometry are crucial to sensor response.

Mesoporous materials

The high surface area and open pore structure of mesoporous materials provide an amplified target–receptor interface making them desirable for sensing applications. The pores can be utilized for anchoring or encapsulating optically active probe molecules, growth and support catalytic nanoparticles, and for immobilization and stabilization of proteins. The pore surfaces can also be used to provide sites for adsorption of targets leading to enhanced local concentrations. Nanoreactors can be formed in which analytes are brought into proximity with sensor probes.

B. J. Melde · B. J. Johnson (✉)
Center for Bio/Molecular Science and Engineering,
Naval Research Laboratory,
Washington, DC 20375, USA
e-mail: brandy.white@nrl.navy.mil

Mesoporous structures can enable rapid diffusion of analytes across a large surface area, resulting in reduced response times. They can also be used to discriminate analytes, for example, on the basis of size or solubility. Recent reviews have focused on mesoporous materials in inorganic sensing [1], anion detection [2], colorimetric and fluorimetric chemical sensing [3, 4], biosensing [5, 6], gas sensing [7], electrochemical analysis [8, 9], and more diverse applications [10–12].

A large amount of work has focused on the synthesis and adaptation of silicates with ordered or semi-ordered pore structures generated through templating with macro-molecular assemblies of amphiphiles. Some of those more commonly employed include alkylammonium surfactants [13, 14] and alkylene oxide block copolymers [15, 16], for example those utilized in MCM-41 and SBA-15 syntheses, respectively. Surfactant micelles self-assemble with a metal oxide precursor (or multiple precursors) to form a nano-composite with the amphiphilic molecules acting as space-fillers in a channel or cage structure. These structures may have varied geometric organization, for example 2D hexagonal and 3D cubic. Removal of the template by calcination or solvent extraction opens the structure, yielding uniformly sized mesopores. As defined by IUPAC, a mesopore has a diameter between 2 and 50 nm. In the materials described here, they are typically less than 10 nm, because of the size of the surfactants used in the syntheses. Micropores and macropores are of sizes that are less than 2 nm and greater than 50 nm, respectively.

In addition to amphiphile templating, mesopores can be generated through replication, or "hard" templating. In this approach, a meso-structured material is used to mold a material of a different composition. In one example, an ordered mesoporous carbon (OMC) is prepared by infiltration of a carbon precursor into a mesoporous silica then pyrolysis [17]. This process is followed by dissolution of the silica with hydrofluoric acid or a strong base leaving an open framework behind. Other processes such as drying a sol–gel or sintering nanoparticles may lead to mesopore formation. These materials, while typically lacking an ordered pore structure, do provide desirable increased surface areas.

In addition to mesoscale morphology and order, control of macroscale morphology has long been of interest in mesoporous materials research. It is also a major consideration for applications. Ordered mesoporous silicas, in particular, have been synthesized as powder precipitates [13, 15], monoliths [18, 19], thin films [20, 21], spherical nanoparticles [22], and various shapes including fibers [23] and nanorods [24]. The bulk morphology affects the types of measurements that can be conducted and the robustness of the material. It can also affect diffusion through the materials and accessibility of the mesostructure. We have only described techniques for the synthesis of mesoporous materials in general terms. For further information, another recent review focusing on template-directed porous electrodes in electrochemical analysis [25] provides a thorough explanation of characterization techniques and a detailed discussion of routes for synthesis. The review also illustrates a number of electrochemical applications.

Metal cation detection

In metal cation sensing, mesoporous materials are applied as scaffolds for the support of functional compounds that provide recognition and signal transduction. The compounds used to accomplish these tasks are as varied as those used in other metal cation-sensing applications. Here, we will not focus on the particular compounds used, but rather on the aspects that are particular to mesoporous materials. Several efforts have focused on the functionalization of mesoporous materials, particularly silicates, for optical detection of a variety of metal cations. Using various optical indicators, limits of detection in nanomolar ranges have been reported, and the materials employed display rapid (typically less than 3 min) color changes on interaction with targets [26], The pore geometry and particle morphology of the probe sinks have been shown to be major factors in sensing efficiency [27, 28]. Monolithic mesoporous materials featuring relatively large particle morphologies were shown to provide higher loading capacities than precipitated powder SBA-15 for optical probes. These higher capacities (i.e., increased number of binding sites) resulted in lower limits of detection. When monolithic materials of different meso-structure were compared, those with 3D cubic mesostructures had faster response times than those with 2D hexagonal channels or disordered channels, possibly owing to improved accessibility and efficient metal ion transport [27, 29, 30].

Some recent efforts have focused on adapting materials for use in membrane-type constructs. This format is desirable for achieving more rapid response characteristics. Mesoporous silica supports have been cast as disk-like membranes (~0.05 cm thick) reducing the average diffusion distance to probe molecules [31–33]. The format is also convenient to handle and can provide colorimetric detection that is visible to the eye in the parts per million range. Nanocrystalline mesoporous titania films fabricated from nanoparticles have been applied similarly [34–36]. In these materials, regeneration was accomplished through treatment with potassium iodide. These types of materials were demonstrated to provide the basis for both optical and electrochemical detection of metal cations. Similar applications have been developed using functionalized mesopo-

rous alumina films [37]. The potential for cell imaging using meosporous silica particles has also been demonstrated as a result of the control over morphology. Schiff base-modified materials with selectively for zinc cations have been applied to detection within human melanoma and HeLa cells after endocytosis of the particles [38].

In addition to macro-morphology, interaction of the probes with the pore surface is an important consideration in the application of mesoporous materials to metal cation sensing. Optical probes are commonly grafted to mesoporous silica through functionalizing dyes with alkoxysilane groups or activating the silica surface by grafting silanes bearing functional groups (Fig. 1) [39]. Alternatives to covalent linkage of the probes take advantage of short-range van der Waals and hydrogen-bonding interactions between abundant silanols on a silicate surface and heteroatoms in a probe molecule (Fig. 1) [26, 40]. Probe molecules with long, hydrophobic alkyl chains, for example, resist leaching from a mesoporous scaffold in an aqueous environment as a result of these interactions.

Probes immobilized in this way have been applied to the detection of a number of metals [29]. Another approach utilizing non-covalent probe incorporation involves first dispersing a cationic surfactant throughout the mesopores. The dye is then loaded into the material through interaction with the surfactant (Fig. 1). This approach has been shown to result in a high loading capacity for probe molecules while maintaining flexibility for metal–probe interactions [30]. The approach may also enhance diffusion through the materials as a result of the difference in the surface-associated mobile layer [41]. Systems of this type have good selectivity in the presence of tens to several-hundredfold concentrations of potentially interfering ions. Regeneration of the materials using stripping agents was demonstrated, however, sensing efficiencies were observed to decrease with repeated use.

Meso-morphology can also be of critical importance to cation-sensing applications. Mesoporosity in a material yields enhanced surface area which provides the potential for an effectively increased localized concentration. In
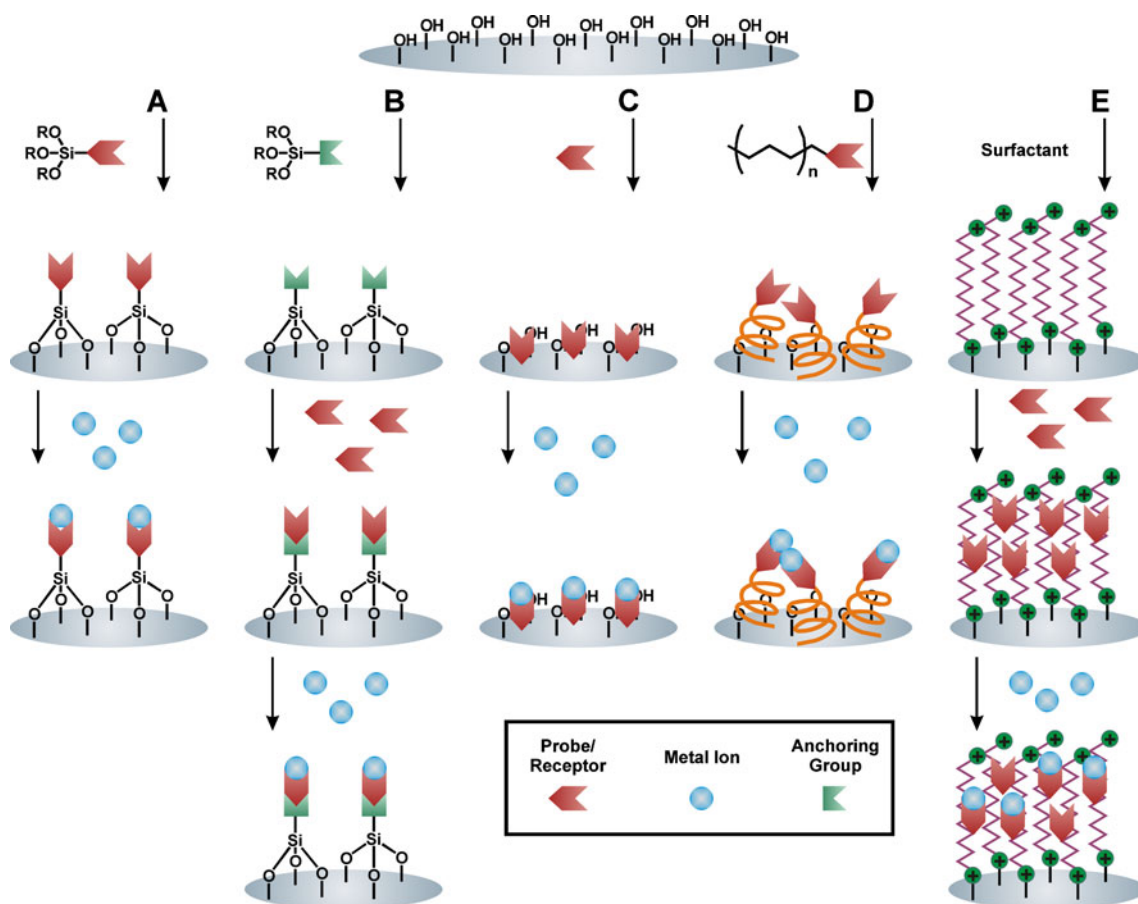
Fig. 1 Functionalization of mesoporous materials. Silane grafting: grafting of probes to mesopore surfaces is accomplished through modification of the probe/receptor (a) or through modification of the mesopore surface to provide a functional group for attachment (b) [39]. Adsorption of probes: probes/receptors are immobilized on the surface through short-range van der Waals and hydrogen-bonding interactions (c), for example, the interaction of hydrophobic alkane chains with the surface (d) [26, 29, 40]. Ionic interactions: probes/receptors are immobilized on the surface through ionic interactions with a cationic surfactant (e) [30]

many cases, this effective concentration alone is enough to provide improved detection characteristics over non-porous materials, for example silica particles [42, 43]. Mesoporosity has also been shown to facilitate interactions between multiple functional groups within the pore structure yielding the potential for novel detection schemes (Fig. 2). In one example, the concave nature of the mesopore was utilized to provide interaction of surface immobilized thiol-groups with indicator molecules. Interaction of a mercury cation displaced the indicator providing a detectable signal [44]. This mechanism could not be utilized in the absence of the concave surfaces of the mesopores, for example, in similarly functionalized activated silica gel or fumed silica.

Another example of the utility of meso-morphology is the generation of a Schiff base on a silica surface through creative co-condensation of silanes [38, 45, 46]. This approach was applied to copper and zinc cation sensing. Functionalization of a mesoporous silica with pyrene derivatives has been used for copper sensing via similar organization [47]. In this material, EPR studies indicated that Cu^{2+} coordinated to the nitrogen atoms of amine groups and oxygen atoms of carboxylic acid groups between two anchored fluorophores and oxygen atoms of silanols or water molecules at the silicate surface to form a distorted octahedron.

A final aspect of mesoporous materials with utility in cation sensing is the potential for "surface imprinting" of the materials. This technique has been applied to the preconcentration of trace levels of metal ions for subse-

quent detection by other methods [48]. The imprinting process involves synthesis of the material with the appropriate targets in place. After removing the metal ion with acid, the surface of the material is left with sites that are complementary to the target. Imprinted materials can show significantly enhanced selectivity in competitive binding studies and often have a higher adsorption capacity than materials synthesized identically in the absence of target (Fig. 2) [49–51].

Anion detection

Anion sensing utilizes many of the features applicable to cation sensing, however, these types of applications do offer some unique examples of mesopore utility. Carboxylate sensing in solution can be accomplished by reaction of phenoxazinone dye with carboxylates of varied chain length. Through a combination of modifications to mesopore surfaces, it is possible to engineer selectivity for longer (more hydrophobic) carboxylates over those that are of short or medium chain lengths (more hydrophilic). The approach involves multi-step functionalization of a mesoporous silica with a dye followed by altering the wetting characteristics of the surface using hexamethyldisilazane [52]. The hydrophobic nature of the resulting material acts to exclude more hydrophilic compounds providing enhanced selectivity for long-chain carboxylates. In this example, the mesopores provide an environment which can be controlled to yield enhanced indicator function. This approach has been applied with variations in several detection schemes. A dye-displacement assay was developed in mesopores loaded with a dye and guanidinium groups. This material favored citrate interaction over that of other carboxylates [53], Similarly functionalized fumed silica yielded a poor signaling response, indicating that the cylindrical mesopores enhanced the coordination of analyte and binding groups. A dye-displacement assay for borate was achieved by loading a mesoporous material with a dye bearing a boronic acid and mannose. The approach has also been applied through using a single dye in materials loaded with a variety of groups for example amino, guanidinium, urea, imidazolium, or quaternary ammonium [54]. Different analytes showed different strengths of dye displacement in these materials, depending on the nature of electrostatic and/or hydrogen bonding between analyte and surface group.

Other reports offer evidence that the mesopore surface without modification can provide useful characteristics. Hydrogen bonding of dyes and analytes with a mesoporous silica surface can contribute to selectivity of the reporter molecules. The surfaces can also contribute to selective quenching interactions [55, 56]. Mesoporous titanium
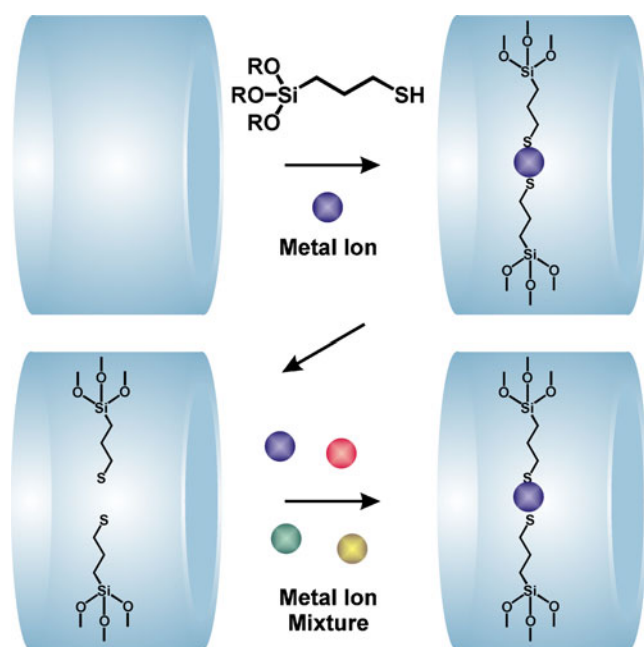
Fig. 2 Mesopore morphology. The concave nature of the mesopore offers novel interactions such as that utilized in a surface imprinting technique [44, 48]

dioxide can provide buffering action that limits or negates the impact of changes in pH on the function of dye molecules [57]. The nanocrystalline films are highly hydroxylated with a point of zero charge at approximately pH 5.5. As in the previous examples, this provides an effectively controlled environment for the function of the dye reporters without the need for multiple functionalization steps.

Amine detection and biosensing

In an approach similar to that described above for carboxylate sensing, mesoporous silicate materials have been used for selective recognition of amines. The surface of the mesoporous material was made hydrophobic before loading with an indicator. The result was a material sensitive to the presence of medium-chain-length primary amines [58]. In this case, the selectivity of the sensing scheme was affected both by the hydrophobic nature of the mesopores and the pore size. The hydrophobic character of the pores worked to exclude short-chain amines while the pore size worked to exclude long-chain amines. A similar approach was used for semi-selective amine detection in a microporous zeolite [59]. The approach has also been used for semi-selective detection of biogenic amines such as histamine, putrescine, and cadaverine in complex matrices [60]. Materials utilizing this approach have been applied in composite systems also, for example, as a mixture containing hydrophilic polyurethane for optical detection of amines [61]. This type of control over interactions within the mesopores can also be used to enhance the sensitivity of electrochemical detection schemes. The enhancement often relies on providing locally increased concentrations of target in proximity to the electrode [62].

Mesoporous metal oxides are often applied at electrode surfaces to enhance electrochemical detection. In addition, mesoporous materials are frequently used to provide stability to proteins. An example in which these attributes were combined involved the encapsulation of glucose oxidase (GOx) in a composite of mesoporous titania, carbon nanotubes, Nafion, and Pt nanoparticles [63]. In addition to the enhanced long-term stability provided by encapsulation, the rapid response time of the resulting system was attributed to the mesopore morphology. An alternative to encapsulation of proteins is their immobilization within the mesopore framework. Immobilization can be accomplished by adsorption of the protein to the mesopore surface or through its covalent linkage to the material. Formaldehyde dehydrogenase was adsorbed on a relatively large-pore (8.0 nm) silica for stabilization of the reagent for use in amperometric detection of aqueous formaldehyde [64]. Encapsulation or immobilization can

also offer stability to inorganic components in a sensing scheme. Silver nanoparticles that were grown inside ordered silicate mesopores (encapsulation) for use in a composite coating applied to electrocatalytic detection of H_2O_2 were stabilized, enabling their extended storage [65]. In contrast, electrodes utilizing bulk silver were found to rapidly decay.

An example of materials synthesized using the replication process described earlier is ordered mesoporous carbons (OMCs). These materials are synthesized using mesoporous silica templates and have been utilized as electrode modifiers for selective electrochemical detection. The presence of OMC provides oxygen-containing surface groups and edge plane-like defect sites can facilitate electron transfer [66, 67]. The activity of this type of product can be further improved by encapsulating cobalt oxide nanoparticles in the pore walls of OMC [68]. The intrinsic conductivity and high surface area provide faster electron kinetics and enhanced current response for oxidation of compounds compared with bare glassy carbon (GC) and Nafion/GC electrodes [69]. Other OMC-modified electrodes have also been described [70], including an OMC/mineral oil paste mixture in which GOx was encapsulated [71].

The combination of mesoporous materials and phospholipid bilayers provides a unique type of sensing scheme. In a pH sensor, as-synthesized (surfactant not extracted) mesostructured silica and photocalcined mesoporous silica films were modified with lipids [72]. A phospholipid bilayer containing gramicidin dimers was formed over the mesopore structure of the silica. Gramicidin enables proton transport through the lipid bilayer. The surrounding alkyl-chain-functionalized sections of the mesoporous material (hydrophobic) contained a pH-sensitive fluorophore and acted as reporter regions. Here, the mesoporous scaffold acts to stabilize the lipid membrane and, together, those components provide a controlled environment for the reporter molecule. In another controlled-access application of mesoporous materials, biotin-functionalized silica was added to planar bilayer lipid membranes for sensing avidin [73]. In this case, the silica material provided transport into the membrane of avidin. Avidin binding by the immobilized biotin resulted in pore blockages yielding a decrease in observed current through the membrane.

Detection of other small molecules in solution

An effective approach for adding binding selectivity for small molecules in mesoporous materials is surface "imprinting". The idea is similar to the imprinting process described for metal cation sensing. In this approach, target or target analog is incorporated into the synthetic process so

that the surfaces of the pores are in contact with the structures during formation (Fig. 3). Although the process is not as specific as molecular imprinting of polymers, it has been shown to provide enhanced sensitivity and selectivity for targets of interest. Incorporation of binding affinity into a mesoporous material can also be accomplished through selection of the compounds making up the pore walls of the material. Mesoporous organosilicas, for example, combine organic "bridging" groups with silica moieties to yield binding characteristics typically associated with polymers while maintaining the rugged character expected of a silica material. Some examples of these materials incorporate benzene and diethylbenzene bridging groups (DEB) between Si atoms in the pore walls. These types of materials have been utilized with and without the imprinting technique. In one example, a sacrificial analogue of 2,4,6-trinitrotoluene (TNT), decylaminetrinitrobenzene, was incorporated with the surfactant template. This type of DEB-silica was used for preconcentration of TNT before electrochemical detection and was also impregnated with a porphyrin for fluorescence sensing of TNT, *p*-cresol, and *p*-nitrophenol [74, 75]. The non-imprinted version of the material demonstrated changes in fluorescence on exposure to solvent vapor. A variation on this approach using surfactant micelles consisting of the surfactant and a percentage of surfactant modified with a target analog at the head group was applied to preconcentration of TNT before HPLC analysis. This type of target analog was found to be more effective in imprinting the organosilicate material than the decylaminetrinitrobenzene [76, 77]. In an approach that bridges those of molecularly imprinted

Fig. 3 Imprinted mesopores. Imprinted surfaces result from self-assembly or condensation in the presence of a target analog [74–77]

polymers and imprinted silicates, ethylenediaminetetraacetic acid (EDTA)–silane, terbium (Tb^{3+}), and sacrificial methyl salicylate (MES) molecules have been incorporated into the synthesis of a silica material. The resulting material was applied to optical detection of MES, a model compound used for sarin [78]. Energy transfer between analyte MES and Tb nanocrystals in the mesopores led to intense fluorescence emission as compared with other nerve gas analogues; this selectivity was not observed in a material prepared without MES.

Several mesoporous materials applications related to small solvent sensing have utilized the confined nature of the environment within the pores to enhance sensing capabilities. An ordered mesostructured silicate templated with a surfactant containing an anthracene group at its tail end was applied to fluorescence detection of solvents [79]. Intermolecular π–π interactions from partially overlapped anthracene molecules in the as-synthesized (surfactant not extracted) material resulted in fluorescent excimer emission. When the material was placed in a polar solvent, for example dimethlyformamide, emission resembled monomer emission. Alternatively, in the presence of a non-polar solvent, for example hexane, anthracene molecules aggregated and fluorescence emission was quenched. Dendrimer confinement within the pores of a mesoporous titania film was utilized for detection of phenolic compounds [80]. The increased proximity of dendrimers and targets within the mesopores facilitated hydrogen bonding between analytes and dendrimers leading to enhanced sensitivity over dendrimers in free solution. The small binding pocket size has also been suggested to affect resorcinol selectivity in a mesopore system [81].
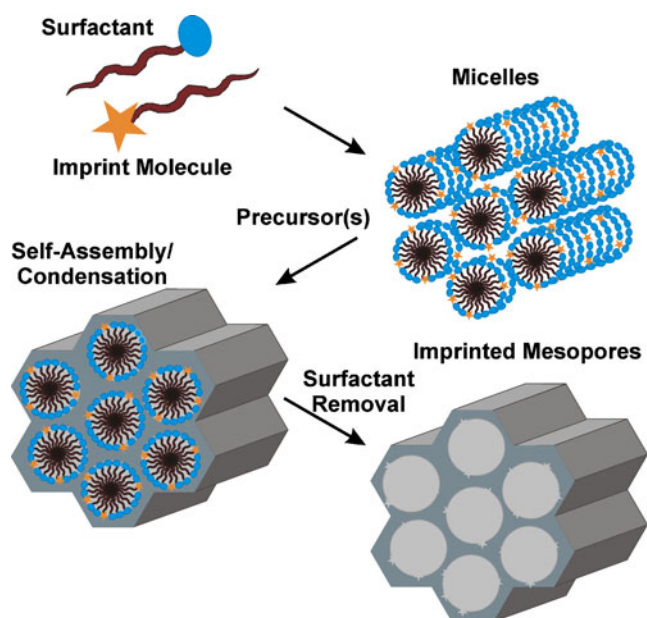
Gas detection

As in applications directed at other types of targets, the macro and meso-scale morphologies of mesoporous materials strongly affect their utility in the detection of light gases. In systems employing electrical conductivity, tin oxide-based mesoporous materials are commonly used. The semiconducting metal oxide enables oxidation/reduction of gas molecules at the material surface. As a result, surface morphology is an important factor in sensitivity. A good example of this was provided by comparison of tin dioxide (SnO$_2$) films synthesized through chemical precipitation, sol–gel, and dissolution pyrolysis methods [82]. Although the materials had similar small grain sizes, the film fabricated by dissolution pyrolysis was more porous than those synthesized by other methods. This more porous film had improved sensitivity to ethanol and chlorine vapors at lower operating temperatures. In another set of experiments, nanocrystalline SnO$_2$ films were applied to detection

of hydrogen and carbon monoxide. Variations in synthetic approaches yielded greater nanocrystallinity and larger pore sizes as annealing temperatures were increased. Pore sizes in the materials ranged from micropores (1–2 nm) to large mesopores (10 nm) [83]. Improved crystallinity provided faster transport of charge carriers from surface into bulk (and vice versa) while larger mesopores increased diffusion of the reducing gases, hydrogen and carbon monoxide, leading to larger signals. On the other hand, micropores introduced size selectivity for hydrogen over carbon monoxide.

Modification of material composition by incorporation of platinum or gold dopants in SnO_2 films has been demonstrated to increase selectivity for particular targets [84, 85]. Incorporation of different percentages of noble metal doping agents has been shown to lead to differences in the grain sizes of the resulting materials. An increased number of grain boundaries has been correlated with enhanced sensitivity and with an increase in the number of catalytic adsorption sites. Combining palladium doping with alteration in mesopore morphology has been shown to provide selectivity for hydrogen over methane and carbon monoxide [86]. This type of material provided an open, interconnected pore network and the reduced grain size shown to be an important component in the doping approach. The result was an increased rate of SnO_2 reduction over that of other materials.

In materials of other compositions, variation in macro and meso-morphology has been shown to be equally important. Zinc oxide (ZnO) materials with varied meso-morphology and particle interconnectivity were compared for application to ethanol detection [87]. Mesoporous ZnO yielded a better conductometric response to ethanol vapors and provided selectivity over benzene at a lower operating temperatures. Mesoporous TiO_2 films created by sintering anatase nanoparticles were more sensitive than relatively non-porous films formed by chemical vapor deposition [88]. Tin–indium oxide (SnO_2–In_2O_3) composite materials provide enhanced thermal stability over SnO_2 materials. In one such material, an In_2O_3–SnO_2 nanocomposite was precipitated to provide a square morphology with irregular micropores. The performance of this material was superior to that of non-porous nanorod particles when applied to ethanol detection [89]. Mesoporous In_2O_3 nanorods consisting of small, well-aligned nanoparticles were shown to provide an increased number of grain junctions compared with larger grain nanoparticles. This increase yielded greater sensitivity to ethanol vapors with enhanced selectivity [90]. Crystalline iron oxide (α-Fe_2O_3) nanospheres with an unusual mesopore core-shell morphology have also been shown to be significantly more sensitive to ethanol vapor than non-porous α-Fe_2O_3 nanoparticles [91].

Functionalization of mesoporous materials can be used to provide selective gas adsorption, for example, in combination with quartz crystal microbalance (QCM) technology. Mesoporous carbon capsules have been shown to enable preferential uptake of aromatic compounds such as benzene and aniline compared with cyclohexane and ammonia [92], possibly owing to π–π interactions between the material and the targets. Loading these materials with lauric acid provided a method for tuning the target interactions to favor adsorption of ammonia and butyl-amine. Modification of the materials using dodecylamine altered interactions to favor adsorption of acetic acid vapor. Similarly, modification of mesoporous silica films through grafting has been applied to enhancing the sensitivity or selectivity of the materials. Modification using β-cyclodextrin has been applied to enhancing QCM sensing of benzene and ethanol vapors. The mesoporous materials were shown to be advantageous over similarly modified planar substrates [93]. Better selectivity for ethanol was introduced by using triphenylphosphine-modified mesoporous silica. Combining the two materials in a multi-channel array enabled estimation of both benzene and ethanol vapors in a mixture [94].

There are several other examples of silica functionalization for sensing applications. Sensing of nitric oxide using mesoporous silicas has been accomplished through functionalization with cobalt phthalocyanine, which forms a nitrosyl derivative with the gas [95], and guanylate cyclase, a hemoprotein that is the major cellular receptor for NO [96]. Mesoporous silicates have been functionalized with RuO_2 nanoparticles for adsorption and conversion of carbon monoxide and nitrogen dioxide [97]. Boron trifluoride (BF_3) detection was accomplished with selectivity over boron trichloride (BCl_3) using dibenzoylmethane grafting [98]. Selectivity for benzene detection over that of methanol was enhanced by using an ordered benzene-bridged mesoporous organosilica film [99]. Omitting the phenylene bridging groups in the pore walls (more available silanol adsorption sites) resulted in the opposite selectivity.

Conclusions

Mesoporous materials-based sensing applications have emerged over the last ten years. Materials templated with amphiphiles have been of particular interest. Early reports naturally focused on demonstrating the feasibility of using mesoporous supports in sensing and their benefits with regard to signal enhancement owing to surface area and facile diffusion through pores. More recent investigations have been more vigorous in identifying and tailoring the selectivity of mesoporous materials for individual sensing

applications. Mesoporous materials have functioned as adsorbents, reactors, stabilizers, filters, and catalysts to aid a given application. Morphological factors, for example pore size, pore geometry, and macro-morphology, and functional factors, for example incorporated functional groups and pore wall composition, have been combined creatively to tune selectivity and reaction kinetics. Many more reports on the elegant design of mesoporous materials for selective sensing can be expected. Further research is likely to be necessary in the areas of morphological control and incorporation into composites in order to enable optimum integration with devices and sensing platforms. Ongoing efforts directed at understanding surface and interface dynamics at relevant length scales should support the further development and application of these versatile materials.

References

1. Carrington NA, Xue ZL (2007) Acc Chem Res 40:343–350
2. Martínez-Máñez R, Sancenón F (2006) Coord Chem Rev 250:3081–3093
3. Ariga K, Vinu A, Hill JP, Mori T (2007) Coord Chem Rev 251:2562–2591
4. Basabe-Desmonts L, Reinhoudt DN, Crego-Calama M (2007) Chem Soc Rev 36:993–1017
5. Slowing II, Trewyn BG, Giri S, Lin VS-Y (2007) Adv Funct Mater 17:1225–1236
6. Trewyn BG, Giri S, Slowing II, Lin VS-Y (2007) Chem Commun 3236–3245
7. Tiemann M (2007) Chem Eur J 13:8376–8388
8. Walcarius A (2008) Electroanalysis 20:711–738
9. Walcarius A, Kuhn A (2008) Trends Anal Chem 27:593–603
10. Melde BJ, Johnson BJ, Charles PT (2008) Sensors 8:5202–5228
11. Asefa T, Duncan CT, Sharma KK (2009) Analyst 134:1980–1990
12. Walcarius A, Collinson MM (2009) Annual Rev Anal Chem 2:121–143
13. Kresge CT, Leonowicz ME, Roth WJ, Vartuli JC, Beck JS (1992) Nature 359:710–712
14. Beck JS, Vartuli JC, Roth WJ, Leonowicz ME, Kresge CT, Schmitt KD, Chu CT-W, Olson DH, Sheppard EW, McCullen SB, Higgins JB, Schlenker JL (1992) J Am Chem Soc 114:10834–10843
15. Zhao D, Feng J, Huo Q, Melosh N, Fredrickson GH, Chmelka BF, Stucky GD (1998) Science 279:548–552
16. Zhao D, Huo Q, Feng J, Chmelka BF, Stucky GD (1998) J Am Chem Soc 120:6024–6036
17. Ryoo R, Joo SH, Jun S (1999) J Phys Chem B 103:7743–7746
18. Attard GS, Glyde JC, Goltner CG (1995) Nature 378:366–368
19. Melosh NA, Lipic P, Bates FS, Wudl F, Stucky GD, Fredrickson GH, Chmelka BF (1999) Macromolecules 32:4332–4342
20. Yang H, Kuperman A, Coombs N, Mamiche-Afara S, Ozin GA (1996) Nature 379:703–705
21. Lu Y, Ganguli R, Drewien CA, Anderson MT, Brinker CJ, Gong W, Guo Y, Soyez H, Dunn B, Huang MH, Zink JI (1997) Nature 389:364–368
22. Lu Y, Fan H, Stump A, Ward TL, Rieker T, Brinker CJ (1999) Nature 398:223–226
23. Schacht S, Huo Q, Voight-Martin IG, Stucky GD, Schüth F (1996) Science 273:768–771
24. Ji X, Lee KT, Monjauze M, Nazar LF (2008) Chem Commun 4288–4290
25. Walcarius A (2010) Anal Bioanal Chem 396:261–272
26. Balaji T, El-Safty SA, Matsunaga H, Hanaoka T, Mizukami F (2006) Angew Chem Int Ed 45:7202–7208
27. El-Safty SA, Ismail AA, Matsunaga H, Mizukami F (2007) Chem Eur J 13:9245–9255
28. Ismail AA (2008) 2008 317:288–297
29. El-Safty SA, Ismail AA, Matsunaga H, Nanjo H, Mizukami F (2008) J Phys Chem C 112:4825–4834
30. El-Safty SA, Ismail AA, Matsunaga H, Hanaoka T, Mizukami F (2008) Adv Funct Mater 18:1485–1500
31. El-Safty SA, Prabhakaran D, Kiyozumi Y, Mizukami F (2008) Adv Funct Mater 18:1739–1750
32. El-Safty SA (2009) Adsorption 15:227–239
33. El-Safty SA (2009) J Mater Sci 44:6764–6774
34. Palomares E, Vilar R, Durrant JR (2004) Chem Commun 362–363
35. Coronado E, Galán-Mascarós JR, Martí-Gastaldo C, Palomares E, Durrant JR, Vilar R, Gratzel M, Nazeeruddin MK (2005) J Am Chem Soc 127:12351–12356
36. Nazeeruddin MK, Censo DD, Humphry-Baker R, Grätzel M (2006) Adv Funct Mater 16:189–194
37. Reynal A, Albero J, Vidal-Ferran A, Palomares E (2009) Inorg Chem Commun 12:131–134
38. Sarkar K, Dhara K, Nandi M, Roy P, Bhaumik A, Banerjee P (2009) Adv Funct Mater 19:223–234
39. Kim E, Kim HE, Lee SJ, Lee SS, Seo ML, Jung JH (2008) Chem Commun 3921–3923
40. El-Safty SA, Prabhakaran D, Ismail AA, Matsunaga H, Mizukami F (2007) Adv Funct Mater 17:3731–3745
41. van Oudenaarden A, Boxer SG (1999) Science 285:1046–1048
42. Lee MH, Lee SJ, Jung JH, Lim H, Kim JS (2007) Tetrahedron 63:12087–12092
43. Javanbakht M, Divsar F, Badiei A, Ganjali MR, Norouzi P, Ziarani GM, Chaloosi M, Jahangir AA (2009) Anal Sci 25:789–794
44. Ros-Lis JV, Casasús R, Comes M, Coll C, Marcos MD, Martínez-Máñez R, Sancenón F, Soto J, Amorós P, Haskouri JE, Garró N, Rurack K (2008) Chem Eur J 14:8267–8278
45. Gao L, Wang JQ, Huang L, Fan XX, Zhu JH, Wang Y, Zou ZG (2007) Inorg Chem 46:10287–10293
46. Gao L, Wang Y, Wang J, Huang L, Shi L, Fan X, Zou Z, Yu T, Zhu M, Li Z (2006) Inorg Chem 45:6844–6850
47. Kledzik K, Orłowska M, Patralska D, Gwiazda M, Jezierska J, Pikus S, Ostaszewski R, Kłonkowski AM (2007) Appl Surf Sci 254:441–451
48. Wang L, Zhou M, Jing Z, Zhong A (2009) Microchim Acta 165:367–372
49. Dai S, Burleigh MC, Shin Y, Morrow CC, Barnes CE, Xue Z (1999) Angew Chem Int Ed 38:1235–1239
50. Fang G-Z, Tan J, Yan X-P (2005) Anal Chem 77:1734–1739
51. Fan Z (2006) Talanta 70:1164–1169
52. Descalzo AB, Rurack K, Weisshoff H, Martínez-Máñez R, Marcos MD, Amorós P, Hoffmann K, Soto J (2005) J Am Chem Soc 127:184–200
53. Comes M, Rodríguez-López G, Marcos MD, Martínez-Máñez R, Sancenón F, Soto J, Villaescusa LA, Amorós P, Beltrán D (2005) Angew Chem Int Ed 44:2918–2922

54. Comes M, Aznar E, Moragues M, Marcos MD, Martínez-Máñez R, Sancenón F, Soto J, Villaescusa LA, Gil L, Amorós P (2009) Chem Eur J 15:9024–9033

55. Kim E, Kim HJ, Bae DR, Lee SJ, Cho EJ, Seo MR, Kim JS, Jung JH (2008) New J Chem 32:1003–1007

56. Seo SM, Cho EJ, Lee SJ, Nam KC, Park S-H, Jung JH (2008) Micropor Mesopor Mater 114:448–454

57. Palomares E, Vilar R, Green A, Durrant JR (2004) Adv Funct Mater 14:111–115

58. Comes M, Marcos MD, Martínez-Máñez R, Sancenón F, Soto J, Villaescusa LA, Amorós P, Beltrán D (2004) Adv Mater 16:1783–1786

59. Comes M, Marcos MD, Martínez-Máñez R, Millán MC, Ros-Lis JV, Sancenón F, Soto J, Villaescusa LA (2006) Chem Eur J 12:2162–2170

60. García-Acosta B, Comes M, Bricks JL, Kudinova MA, Kurdyukov VV, Tolmachev AI, Descalzo AB, Marcos MD, Martínez-Máñez R, Moreno A, Sancenón F, Soto J, Villaescusa LA, Rurack K, Barat JM, Escriche I, Amorós P (2006) Chem Commun 2239–2241

61. Comes M, Marcos MD, Martínez-Máñez R, Sancenón F, Villaescusa LA, Graefe A, Mohr GJ (2008) J Mater Chem 18:5815–5823

62. Wang F, Yang J, Wu K (2009) Anal Chim Acta 638:23–28

63. Choi HN, Han JH, Park JA, Lee JM, Lee W-Y (2007) Electroanalysis 19:1757–1763

64. Shimomura T, Itoh T, Sumiya T, Mizukami F, Ono M (2008) Sens Actuators B 135:268–275

65. Lin D-H, Jiang Y-X, Wang Y, Sun S-G (2008) J Nanomater 2008:1–10

66. Zhou M, Ding J, Guo L-P, Shang Q-K (2007) Anal Chem 79:5328–5335

67. Ndamanisha JC, Bai J, Qi B, Guo L (2009) Anal Biochem 386:79–84

68. Hou Y, Ndamanisha JC, Guo L-P, Peng X-J, Bai J (2009) Electrochim Acta 54:6166–6171

69. Zhou M, Guo L-P, Hou Y, Peng X-J (2008) Electrochim Acta 53:4176–4184

70. Hu G, Ma Y, Guo Y, Shao S (2009) J Electroanal Chem 633:264–267

71. Zhu L, Tian C, Zhu D, Yang R (2008) Electroanalysis 20:1128–1134

72. Yang T-H, Yee CK, Amweg ML, Singh S, Kendall EL, Dattelbaum AM, Shreve AP, Brinker CJ, Parikh AN (2007) Nano Lett 7:2446–2451

73. Nozawa K, Osono C, Sugawara M (2007) Sens Actuators B 126:632–640

74. Trammell SA, Zeinali M, Melde BJ, Charles PT, Velez FL, Dinderman MA, Kusterbeck A, Markowitz MA (2008) Anal Chem 80:4627–4633

75. Johnson-White B, Zeinali M, Shaffer KM, Patterson CHJ, Charles PT, Markowitz MA (2007) Biosens Bioelectron 22:1154–1162

76. Johnson BJ, Melde BJ, Charles PT, Cardona DC, Dinderman MA, Malanoski AP, Qadri SB (2008) Langmuir 24:9024–9029

77. Johnson BJ, Melde BJ, Thomas C, Malanoski AP, Leska IA, Charles PT, Parrish DA, Deschamps JR (2010) Sensors 10:2315–2331

78. Smith CB, Anderson JE, Massaro RD, Tatineni B, Kam KC, Tepper GC (2008) Appl Spectrosc 6:604–610

79. Li L-L, Sun H, Bai Y-C, Fang C-J, Yan C-H (2009) Chem Eur J 15:4716–4724

80. Martínez-Ferrero E, Franc G, Mazères S, Turrin C-O, Boissière C, Caminade A-M, Majoral J-P, Sanchez C (2008) Chem Eur J 14:7658–7669

81. Xiao W, Xiao D (2007) Talanta 72:1288–1292

82. Vaezi MR, Sadrnezhaad SK (2007) Mater Sci Eng B 140:73–80

83. Li L-L, Zhang W-M, Yuan Q, Li Z-X, Fang C-J, Sun L-D, Wan L-J, Yan C-H (2008) Cryst Growth Des 8:4165–4172

84. Ramgir NS, Hwang YK, Jhung SH, Mulla IS, Chang J-S (2006) Sens Actuators B 114:275–282

85. Ramgir NS, Hwang YK, Jhung SH, Kim H-K, Hwang J-S, Mulla IS, Chang J-S (2006) Appl Surf Sci 252:4298–4305

86. De G, Köhn R, Xomeritakis G, Brinker CJ (2007) Chem Commun 1840–1842

87. Xu H, Liu X, Cui D, Li M, Jiang M (2006) Sens Actuators B 114:301–307

88. Benkstein KD, Semancik S (2006) Sens Actuators B 113:445–453

89. Chu D, Zeng Y-P, Jiang D, Masuda Y (2009) Sens Actuators B 137:630–636

90. Li E, Cheng Z, Xu J, Pan Q, Yu W, Chu Y (2009) Cryst Growth Des 9:2146–2151

91. Chen H, Zhao Y, Yang M, He J, Chu PK, Zhang J, Wu S (2010) Anal Chim Acta 659:266–273

92. Ji Q, Yoon SB, Hill JP, Vinu A, Yu J-S, Ariga K (2009) J Am Chem Soc 131:4220–4221

93. Palaniappan A, Li X, Tay FEH, Li J, Su X (2006) Sens Actuators B 119:220–226

94. Palaniappan A, Su X, Tay FEH (2006) IEEE Sens J 6:1676–1682

95. Palaniappan A, Moochhala S, Tay FEH, Su X, Phua NCL (2008) Sens Actuators B 129:184–187

96. Palaniappan A, Moochhala S, Tay FEH, Phua NCL, Su X (2008) Sens Actuators B 133:241–243

97. Jansat S, Pelzer K, García-Antón J, Raucoules R, Philippot K, Maisonnat A, Chaudret B, Guari Y, Mehdi A, Reyé C, Corriu RJP (2007) Adv Funct Mater 17:3339–3347

98. Banet P, Legagneux L, Hesemann P, Moreau JJE, Nicole L, Quach A, Sanchez C, Tran-Thi T-H (2008) Sens Actuators B 130:1–8

99. Yuliarto B, Kumai Y, Inagaki S, Zhou H (2009) Sens Actuators B 138:417–421